high (~10-20) rotational angular momentum. In order to understand this reaction better, we have begun to look at the accurate quantum dynamics on a potential energy surface[96] with a realistic exit valley. Our reaction probabilities[22] for $j = J = 0$ are in satisfying agreement with independent calculations[30] performed simultaneously by Pack and co-workers. The accurate quantal results[22,30] show no resonances for total angular momentum zero in the entire experimental energy range, in encouraging agreement with the interpretation[92,94] that the resonance occurs only at higher J. (Note: resonances *have* been found theoretically for $J = 0$ at higher energies.[30]) Furthermore, the accurate quantum dynamics show that at threshold a significant fraction of the reaction products are in the $v' = 3$ vibrational level, in good agreement with experiment. Because the thresholds for individual v' are sensitive to effective barriers[97] of the type discussed above for the $O + H_2$ reaction, it is particularly exciting to have accurate quantum dynamics calculations of this threshold behavior.

We have also calculated converged reaction probabilities and collisional delay times for $F + H_2$ collisions with nonzero rotational angular momentum and nonzero total angular momentum.[22,23] The time delays show that the contribution of longer lived collisions is relatively greater for certain subsets of final states. Future work on this system will allow us to test the sensitivity of the results to proposed improvements[98] in the potential energy surface.

(95) For a picture of what these might look like, see: Thompson, T. C.; Truhlar, D. G. *J. Phys. Chem.* **1984**, *88*, 210.
(96) Steckler, R.; Schwenke, D. W.; Brown, F. B.; Truhlar, D. G.; Garrett, B. C. *J. Chem. Phys.* **1985**, *82*, 188. Steckler, R.; Truhlar, D. G.; Garrett, B. C. *J. Chem. Phys.* **1985**, *82*, 5499.
(97) Steckler, R.; Truhlar, D. G.; Garrett, B. C.; Blais, N. C.; Walker, R. B. *J. Chem. Phys.* **1984**, *81*, 5700.
(98) Schwenke, D. W.; Steckler, R.; Brown, F. B.; Truhlar, D. G. *J. Chem. Phys.* **1986**, *84*, 5706.

Conclusions

We see that the area of accurate treatments of three-dimensional quantum mechanical atom-plus-diatom scattering is reaching the point where many exciting applications can be made. Although several systems have been treated, the number of interesting questions remaining is far greater. In addition to the need for further calculations on the systems that have already been considered, there are two future areas of pursuit for this research effort. First is the application to new systems. This includes reactive systems not yet studied as well as other kinds of systems where the efficiency of algebraic variational methods may also be exploited, such as electron scattering, photochemical reactions, and photodissociation. The other area is in improvements of the method. The latter goal can be achieved both by increasing the efficiency of the calculation for a given basis set and by reducing the basis set size required for a given accuracy. We look forward to both kinds of advances.

Acknowledgment. We are grateful to David Chatfield, Philippe Halvick, Kenneth Haug, Mirjana Mladenovic, Omar Sharafeddin, Yan Sun, Chi-hui Yu, John Zhang, Yici Zhang, and Meishan Zhao for invaluable contributions to this research. This work was supported in part by the National Science Foundation and Minnesota Supercomputer Institute.

ARTICLES

Theoretical Study of the Quenching of the Low-Lying Excited States of Li and Mg by CH_4

P. Chaquin,* A. Papakondylis, C. Giessner-Prettre, and A. Sevin

Laboratoire de Chimie Organique Théorique (URA 506), Université Pierre et Marie Curie, Bâtiment F, 4, place Jussieu, 75252 Paris Cedex 05, France *(Received: June 6, 1989; In Final Form: February 2, 1990)*

The reactivity of the ground state (GS) and the low excited states of Li and Mg atoms with CH_4 has been studied on the basis of SCF-CI ab initio calculations. No attractive surface is found starting from ^2S (GS) and ^2P states of Li and ^1S, ^3P, and ^1P states of Mg. No energy barrier above endothermicity is found for the $CH_4 + M \rightarrow CH_3 + MH$ reactions in the case of Li, for both insertion and abstraction model mechanisms. In the case of Mg, the relative height of energy barriers indicates that the insertion mechanism is preferred when starting from the ^1P state. The existence of a CH_3·MgH bent exciplex with a small singlet-triplet gap accounts for a possible intersystem crossing. Some consequences and a comparison with H_2 are discussed concerning the physical and chemical quenching of the excited metal atoms.

Introduction

The quenching of the low-lying excited states of alkali and alkaline-earth metals by diatomic or small molecules constitutes a vast domain of investigation for both experimentalists and theoreticians.[1] For all these systems, the low-lying excited states of the metal lie below those of the interacting molecule. It is well established that, in the excited states, two kinds of quenching might be observed: (i) chemical quenching involving the rupture and formation of bonds; (ii) physical quenching where the energy transfer occurs through the formation of exciplexes. Of course these processes are ruled by the thermodynamics and, dealing with strongly bonded molecules, chemical quenching is not very likely to take place since the bonds that might be formed between the metal and other atoms are generally weaker than the bonds that have been cleaved in the initial molecule. It has also been shown that in the formation of exciplexes two types of forces are to be considered. The first one can be depicted in terms of MO in-

(1) Nikitin, E. E. *Theory of Atomic and Molecular Processes in Gases*; Oxford University Press: Oxford, UK, 1974. Klabunde, K. J. *Chemistry of Free Atoms and Particles*; Academic Press: New York, 1980. Breckenridge, W. H. *Reactions of Small Transient Species*; Academic Press: New York, 1983; p 157. Breckenridge, W. H.; Umemoto, H. *Adv. Chem. Phys.* **1982**, *50*, 325. Hertel, I. V. *Adv. Chem. Phys.* **1982**, *50*, 475. Bottcher, C. *Adv. Chem. Phys.* **1980**, *42*, 169.

0022-3654/90/2094-7352$02.50/0

teractions with the p orbitals of the metal leading to an overlap with either σ^* or π^* orbitals of the nonmetallic moiety, thus allowing for an electronic transfer from the metal to the molecule. In response, the molecule, which bears some partial anionic character, stretches for optimizing the bulk effect. This corresponds to the now classical "bond-stretch model" proposed by Hertel et al.[2] The second type of force results from the stabilization of a true charge-transfer species by electronic attraction at short distances. This "ionic model" often referred to as "Nikitin's model"[3] involves the interplay of diabatic covalent and ionic potential surfaces, while in the former model the phenomenon is better understood in terms of classical adiabatic surfaces. For example, a limiting situation is found in the case of Na + H_2[4] and Mg + H_2[5,6] where the bond-stretch model is adequate, while dealing with Li + N_2,[7] Mg + N_2,[8] Na + N_2,[9] Na + HF,[10] or Mg + HF,[11] Nikitin's model is nicely comforted by theoretical investigation by SCF-CI and VB methods. In reality these models are of complementary use: the covalent model is efficient when the negative species resulting from charge transfer is of very high energy and/or when the molecule weakly overlaps with the metal orbitals, such as in the case of Na + H_2; the second model is of concern when the preceding negative moiety resulting from charge transfer is rather stable and has a good overlap with the metal orbitals, such as the case of Li or Mg + N_2.

In dealing with Li or Mg and CH_4, the situation is complex. First of all, the eventual formation at a large distance of stable charge-transfer moieties is ruled out by previous studies that have shown that the additional electron is not bound in CH_4^- (resonant state).[12] An analogy with the previous studies of the Na + H_2 and Mg + H_2 systems is expected, so that the possibilities of physical quenching have to be examined. On the other hand, chemical quenching might be also observed for both metals (i) on the grounds of quantum calculations in the case of Li[13] and (ii) in the case of Mg, due to the relatively high energy of the first excited singlet state and the possible formation of a stable CH_3MgH species. Both processes are endothermic in the ground state (GS). As a matter of fact, it has been shown that, in the gas phase, chemical quenching of the ^1P ($3s^13p^1$) state of Mg yields MgH + CH_3; no production of triplet Mg has been detected.[14-16] On the contrary, recent matrix experiments yielded the insertion product with a strong triplet emission of the Mg atom.[17-19] The most important experimental data will be recalled with more detail in the discussion.

We present here sets of calculated potential energy surfaces (PES's) that take into account the possibilities of physical and chemical quenching.

TABLE I: Calculated Energies (in eV) of the Different States of Reactants and Products, Using Method II

	M + CH_4 (GS)		MH + CH_3 (GS)		$HMCH_3$	
metal	sym	E	sym	E	sym	E
Li[a]	^2S	0.00[b]	$1^1\Sigma^+$	2.83		
	^2P	1.87[c]	$2^1\Sigma+$	5.07		
Mg[d,e]	^1S	0.00[f]	$^2\Sigma^+$	2.87	$^1A_1$	0.85
	^3P	2.57[g]	$^2\Pi$	5.24	$^3A_1$	5.29
	^1P	4.50[h]			^1E	5.70

[a] 10-Å separation. [b] Absolute energy: −47.729 531 au. [c] Experimental value: 1.84 eV.[29] [d] 5-Å separation in the case of Mg + CH_4. [e] 4-Å separation in the case of MgH + CH_3. [f] Absolute energy: −239.926 111 au. [g] Experimental value: 2.72 eV.[29] [h] Experimental value: 4.46 eV.[29]

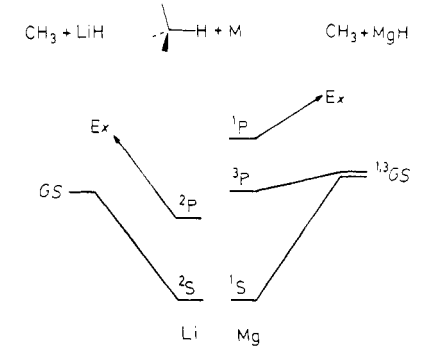

Figure 1. Schematic correlations of GS and low-lying excited states of M + CH_4 → MH + CH_3 reaction.

Methodology

Ab initio SCF-CI caculations have been carried out. The following basis sets were used:[20] 6-31G plus Rydberg functions for Li; 6-31G* plus diffuse functions for Mg; standard 6-31G for H. With C, a problem arises regarding the choice of diffuse functions. By adding to the 6-31G basis a set of sp orbitals that minimizes the CI energy of the lowest Rydberg state, one gets CH_4^- species that are far more too stable. Upon variation of the corresponding Gaussian exponent, we have observed that the CI energy is roughly linearly dependent on the exponent value, tending toward that of CH_4 when decreasing its magnitude. This shows that the extra electron is not bound to CH_4, for if we give it a space that is large enough, we get in reality the energy of CH_4 alone. We thus had to adopt a compromise, by taking an exponent of 0.08, which remains adequate for the calculation of the low-lying PES's without introducing charge-transfer artifacts but nevertheless allowing for a good polarization of the system.[12] The calculations have been achieved in two steps. In the first one, exploratory runs were done with the use of a limited CI space including around 100 configurations (method I). The SCF step was achieved by using the MONSTERGAUSS series of programs.[21] The Davidson RHF Hamiltonian[22] was used for doublet species and radical pairs; the closed shell Roothaan[23] Hamiltonian was used in the other cases. The energies of the crucial points were then refined through a Møller–Plesset[24] (MP) CI, using the CIPSI method.[25] A set of around 80–100 reference configurations was

(2) Hertel, I. V. *Progress in Electronic-to-Vibrational Energy Transfer in Dynamics of the Excited States*; Lawley, K. P., Ed.; Wiley: New York, 1982.
(3) Bjerre, A.; Nikitin, E. E. *Chem. Phys. Lett.* **1967**, *1*, 179.
(4) Chaquin, P.; Sevin, A. *Chem. Phys.* **1985**, *93*, 49. Yarkony, D. R. *J. Chem. Phys.* **1986**, *84*, 3706.
(5) Chaquin, P.; Sevin, A.; Yu, H. T. *J. Phys. Chem.* **1985**, *89*, 2813. Lengsfield, B. H.; Sax, P.; Yarkony, D. R. *J. Chem. Phys.* **1984**, *81*, 4549.
(6) Blickensderfer, R. P.; Jordan, K. D.; Adams, N.; Breckenridge, W. H. *J. Phys. Chem.* **1982**, *86*, 1930.
(7) Sevin, A.; Chaquin, P.; Hamon, L.; Hiberty, P. C. *J. Am. Chem. Soc.* **1988**, *110*, 5861.
(8) Chaquin, P.; Sevin, A. *Chem. Phys.* **1988**, *123*, 351.
(9) Habitz, P. *Chem. Phys.* **1980**, *54*, 131.
(10) Sevin, A.; Hiberty, P. C.; Lefour, J.-M. *J. Am. Chem. Soc.* **1987**, *109*, 1845.
(11) Chaquin, P. *J. Phys. Chem.* **1987**, *91*, 440.
(12) Komhia, N.; Daudey, J.-P.; Malrieu, J.-P. *J. Phys. B: At. Mol. Phys.* **1987**, *20*, 4375.
(13) McCaffrey, J. G.; Poirier, R. A.; Ozin, G. A.; Csizmadia, I. G. *J. Phys. Chem.* **1984**, *88*, 2898.
(14) Breckenridge, W. H.; Umemoto, H. *J. Chem. Phys.* **1984**, *81*, 3859.
(15) Breckenridge, W. H.; Umemoto, H. *J. Chem. Phys.* **1984**, *80*, 4168.
(16) Breckenridge, W. H.; Umemoto, H. *J. Chem. Phys.* **1981**, *75*, 698.
(17) McCaffrey, J. G.; Ozin, G. A. *J. Chem. Phys.* **1988**, *89*, 1839.
(18) McCaffrey, J. G.; Ozin, G. A. *J. Chem. Phys.* **1988**, *89*, 1844.
(19) McCaffrey, J. G.; Parnis, J. M.; Ozin, G. A. *J. Chem. Phys.* **1988**, *89*, 1858.
(20) Francl, M. M.; Pietro, W. J.; Hehre, W. J.; Binkley, J. S.; Gordon, M. S.; Defrees, D. J.; Pople, J. A. *J. Chem. Phys.* **1982**, *77*, 3654. Gordon, M. S.; Binkley, J. S.; Pople, J. A.; Pietro, W. J. *J. Am. Chem. Soc.* **1982**, *104*, 2997. Pietro, W. J.; Francl, M. M.; Hehre, W. J.; Defrees, D. J.; Pople, J. A.; Binkley, J. S. *J. Am. Chem. Soc.* **1982**, *104*, 5039.
(21) Binkley, J. S.; Whiteside, R. A.; Krishnan, R.; Seeger, R.; Defrees, D. J.; Schlegel, H. B.; Topiol, S.; Kahn, L. R.; Pople, J. A. *Gaussian 80*; *QCPE* **1978**, *No. 368*.
(22) Davidson, E. R. *Chem. Phys. Lett.* **1973**, *21*, 565.
(23) Roothan, C. C. J. *Rev. Mod. Phys.* **1951**, *23*, 69.
(24) Møller, C.; Plesset, M. S. *Phys. Rev.* **1934**, *46*, 618.
(25) Huron, B.; Malrieu, J.-P.; Rancurel, P. *J. Chem. Phys.* **1973**, *58*, 5745. Malrieu, J.-P. *Theor. Chim. Acta* **1982**, *62*, 163. Evangelisti, S.; Daudey, J.-P.; Malrieu, J.-P. *Chem. Phys.* **1983**, *75*, 91.

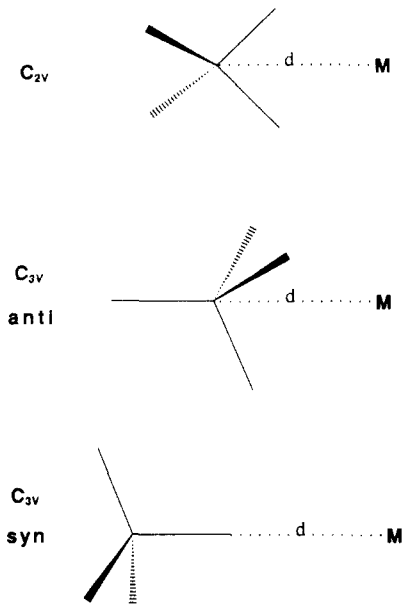

Figure 2. Model approaches of methane and metal atoms.

used as a basis for the multireference perturbation scheme involving 10^6–10^7 terms, according to the state under scrutiny (method II). The exploratory runs (using method I) can be used for a first insight into the PES's shapes, the multireference values being required for a quantitative discussion of the phenomena. In Table I are reported the reference energies obtained by method II. We see that the relative energies obtained by method II are in good agreement with experimental data.

Preliminary Survey of Reactivity

From the data of Table I, several points emerge. First of all, a striking difference between both metals is found regarding the thermodynamics of the feasible chemical processes. (i) With Li, the formation of either a CH_3LiH complex or of separated CH_3 + LiH is endothermic in the GS or starting from the lowest excited state ^2P ($2p^1$). It becomes exothermic with respect to 2^2S ($3s^1$) or higher energy states. (ii) With Mg, the formation of CH_3MgH is exothermic starting from the lowest excited states, either singlet or triplet $^{1,3}P$ ($3s^13p^1$). The reaction remains weakly endothermic in the GS. It is clear that these considerations presume neither the nature and height of potential energy barriers nor the symmetry and multiplicity constraints. In particular, in the case of Mg, the reaction of triplet species implies intersystem crossing with singlet surfaces.

In a first step, let us qualitatively examine the M + CH_4 → MH + CH_3 reactions using the simple correlation analysis of Figure 1. The Mg + CH_4 system (right) can be reduced to a four-electron problem: two coming from the C–H bond and two coming from the metal in its 3s or 3p orbitals. On purpose, the correlations are depicted in a somewhat diabatic way, i.e., by considering that the electrons remain in their initial localization as the reaction proceeds. The resulting pair of radical species, the singlet and triplet arrangements of which are degenerate at large separation, are linked to the GS of Mg + CH_4 and to Mg*($3s^13p^1$) + CH_4, respectively. The singlet ($3s^13p^1$) state is linked to an excited species of the final system. In reality, the actual correlations are not likely to be monotonous for important electronic changes are necessary. With Li, the same type of correlation links the GS of Li + CH_4 with the GS of the final system while the first excited state of Li is linked to CH_3 + LiH*.

The formation of exciplexes or products remains to be considered. For both metals, various limiting geometries have been studied. The geometries of approach can be classified according to three categories as displayed in Figure 2: C_{2v}, where the metal approaches two identical hydrogens, and C_{3v}, where the metal approaches along one C–H bond in either an anti geometry with respect to the hydrogen (M···C–H) or an end-on one (C–H···M). The latter approach is also favorable for the direct abstraction reaction CH_4 + M → CH_3 + MH. During the insertion of the metal atom into a C–H bond, a less symmetrical C_s geometry has been used. It is related to either the C_{2v} or C_{3v} geometries by displacement of the metal atom apart from the symmetry axis, the symmetry plane thus containing the C–H bond under scrutiny and the metal. In what follows, the classical labeling of states has been used: for example, n^1S is the nth singlet state of S symmetry. Nevertheless, n might have been omitted when the corresponding state is the lowest one.

Results

The search for ground- and excited-state MCH_4 complexes/exciplexes, during the approach of the reactants, has been carried out at two calculation levels: (i) at the SCF level, using the optimization programs of the MONSTERGAUSS series, in the GS configuration for Li, and in the three relevant configurations for Mg, closed shell ($3s^2$) and singlet and triplet ($3s^13p^1$) open shells; (ii) by method I (limited CI), for the three model approaches of Figure 2. In the GS, for both metals, all kinds of approaches are repulsive, the least unfavorable being the anti C_{3v} pathway. Several points are noteworthy regarding the excited-state behavior. (i) With Li, no exciplex formation is observed in the lowest 1^2P ($2p^1$) excited state, while it is observed for higher energy states such as 2^2S ($3s^1$) and 2^2P ($3p^1$). A qualitative reason is that the compact valence states of Li, either ^2S or ^2P, suffer at short distance from the electronic repulsion of the C–H bonds, without sufficient overlap of metal AO's with σ^* MO's of CH_4. This overlap becomes significant when more diffuse orbitals of higher energy are involved, as in the case of the 2^2S and 2^2P states of Li. (ii) For Mg, similar trends are observed concerning the low-lying states, and only a very weak stabilization is observed for the 2^1S ($3s^14s^1$) and 2^1P ($3s^14p^1$) states in the anti C_{3v} geometry. (iii) In any case when the C–H bonds are allowed to relax, no important stabilization results, even when the metal is close to the bonding distance of one or more hydrogen atoms. This was not the case when dealing with H_2, where the formation of an exciplex, stabilized by a small H–H stretching, has been demonstrated for both metals.[4-6]

For the chemical quenching, two kinds of chemical reactions will be examined, which are referred to as H abstraction by the metal and metal insertion into a C–H bond.

1. Li + CH_4. H Abstraction. The simplest geometrical model consists of an in-line reaction coordinate, the hydrogen atom being transferred from the carbon to the metal at optimal distance. Upon those conditions, the potential hypersurface mainly depends on the C···H and M···H bond lengths, the pyramidalization of CH_3 only playing a minor energetic role, as shown by the calculations. We have seen, in Figure 1, that no adiabatic surface links the lowest excited states of Li + CH_4 to the GS of the products. From a grid of ca. 30 points (method I), a transition state is found along the GS surface: it corresponds to a Li–H distance of 1.70 Å and a C–H distance of 2.12 Å, with practically tetrahedral angles for the remaining C–H bonds. It can thus be considered as Li–H at its equilibrium bond length interacting with CH_3. Nevertheless, at the method II level, this so-called transition state (TS) vanishes and a monotonous PES is thus obtained. The reaction path can be roughly described as follows: first, a weakly endothermic approach at a 2-Å Li···H separation which requires about 0.5 eV; then, keeping the C–Li distance constant (2.08 Å), H is transferred from the carbon to the lithium; and finally both species are separated one from another, the latter process requiring the major part of the endothermicity (2.83 eV; Figure 3).

The lowest two excited PES's ($^2A_1$ and ^2E, originating from ^2P of Li) increase monotonously along the reaction coordinate (RC) and thus do not deserve comment. In upper excited states, the behavior of the 2^2S ($3s^1$) state is noteworthy. During the approach, a small stabilization occurs, so that a compact situation can be easily reached. Staying on the same surface, separation of the fragments is very endothermic, so that no possible adiabatic reaction can be likely. However, the possibility of diabatic switch from the latter surface to the GS surface remains to be examined. Both surfaces of A_1 symmetry are linked via a matrix element

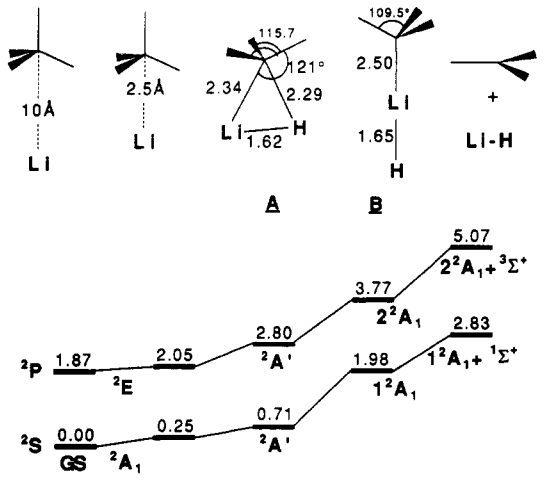

Figure 3. Insertion reaction of Li with CH_4. The energies (in eV) of the main steps (see text) are calculated according to method II.

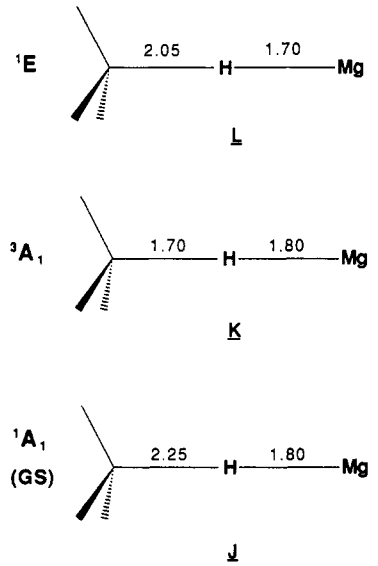

Figure 4. TS structures (method I) for the abstraction reaction $CH_4 + Mg \rightarrow CH_3 + MgH$.

of the form $\langle 1A_1|\partial/\partial q|nA_1\rangle$ having nonzero value when the elementary displacement has the A_1 symmetry.[26] It can therefore be conceived that C–H stretching might afford the corresponding driving force. In such a case, Li–H vibrationally excited, with small rotational excitation energy, would be obtained. A similar analysis of the $3p^1$ components yields a possible diabatic reaction with the LiH states of E symmetry: the coupling displacement now must have the E symmetry, i.e., some distortion from the linear geometry, thus LiH with rotational energy excess would result.

Li Insertion into a C–H Bond. Figure 3 displays the main PES steps of this reaction, obtained by method II, with a reasonable approximation of the RC in the GS. Starting from the preferential C_{3v} approach, at a C–Li distance of 2.5 Å, the reaction proceeds along with a C_s RC, the C–H bond that is of concern and Li determining the symmetry plane. This way, a TS is found, the structure of which has been optimized at the SCF level (structure A of Figure 3). Nevertheless, after MP calculations (method II), this TS no longer exists as can be seen in Figure 3. The important consequence is that there is no stable CH_3LiH species, in contradiction with previous calculations at the SCF level[13] (structure B of Figure 3). With the excited states, all the surfaces have a steep endothermic slope as soon as the insertion process begins, and taking into account the high energy of the excited states of the final system, we see that no adiabatic PES is likely to yield this type of reaction. In the ^2P lowest excited state, an exciplex is found, at the SCF level, with a geometry close to that of structure B. Nevertheless, by method II, the energy barrier for structure A between the reactants and this structure also vanishes. Though structure A is not optimized for the excited state, the existence of a CH_3·LiH exciplex remains very unlikely.

2. Mg + CH_4. H Abstraction. The data displayed in Figure 4 summarize the saddle point geometries obtained by method I in the GS and the lowest excited triplet and singlet states, including the variation of the two main parameters, the Mg–H and C–H distances, as in the case of Li (vide supra). The HCH angles of the CH_3 group have been found equal to their standard values. The resulting geometries of Figure 4 were used in further calculations (method II), the results of which are reported in Figure 5. No energy barrier is found along the GS $1^1A'$ PES at method II level. The saddle point of Figure 4 (Structure J), determined by method I, is lowered at practically the same energy as that of the CH_3 + MgH products. Thus the reaction only requires the 2.87-eV activation corresponding to its endothermicity. From the lowest singlet state, ^1P, although the overall process is exothermic, an energy barrier of 1.5 eV exists in the corresponding $2^1A'$ PES.

Mg Insertion into a CH Bond. The optimization of the RC and search for saddle points are more difficult than in the proceding case of Li. As a matter of fact, the possible formation of a stable insertion product CH_3–Mg–H has now to be taken into account.

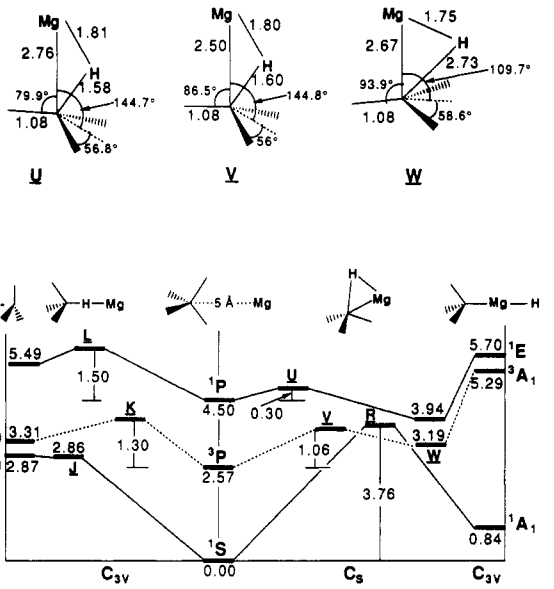

Figure 5. Insertion and abstraction reactions of Mg with CH_4. The energies (in eV) of the different steps are calculated according to method II (see also Figure 6).

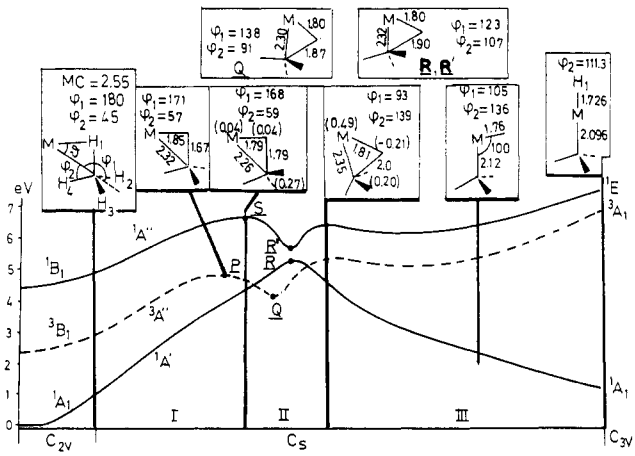

Figure 6. Optimized reaction coordinate (method I) for Mg + CH_4 GS insertion reaction. Numbers in parentheses refer to net atomic charges.

(26) Lee, T. S. *J. Am. Chem. Soc.* **1977**, *99*, 3909 and references therein.

Ground-State Reaction Coordinate. The GS reaction coordinate was optimized, at the SCF level, as follows (Figure 6). Starting from a C_{2v} approach from $d = 4$ Å to $d = 2.55$ Å, the $CMgH_1$ angle (θ) was increased from its initial value in the latter geometry (24.46°) to 180°. For each selected value of this angle, the most relevant parameters were optimized: Mg–H_1 and Mg–C lengths and the ϕ_1 and ϕ_2 angles defined in Figure 6. The resulting RC can be divided into three parts: (i) The first is the endothermic approach of Mg during which the C–H_1 bond does not stretch significantly and the system essentially resembles CH_4 + Mg. We note that the net charge on H_1 is positive whereas it is nearly zero on Mg, yielding small ϕ_2 and large ϕ_1 angles. (ii) The central part of the RC consists of a dramatic angular rearrangement of the system, though the crucial Mg–C and C–H_1 distances undergo only small variations. As the Mg–H bond is formed and the C–H bond is broken, the polarity of H_1 suddenly changes with concomitant increase of ϕ_2 and decrease of ϕ_1. (iii) The third part essentially reflects a stabilization of the insertion product C–H_3–Mg–H through an increase of θ up to 180° (C_{3v} symmetry). (For the latter molecule, we used the optimized geometry parameters published by Jasien and Dykstra.[27]) These geometries were then used for the calculation, according to method I. Then the energy of point R was refined according to method II and is reported in Figure 5.

As expected for a four electron insertion process, which is formally forbidden,[28] the overall reaction requires an activation energy of 3.76 eV and is weakly endothermic (0.84 eV). The transition-state geometry (Figure 6, point R) reveals that the C–H bond length is quite large while the Mg–H bond length is closer to its equilibrium value. By comparison, the linear CH_3–H–Mg structure having similar bond lengths is more stable by nearly 1 eV.

Excited ^1P and ^3P State Reactivity. As landmarks, the curves corresponding to the low-lying states are displayed in Figure 6, in which the abscissa is the GS reaction coordinate. First, it is noteworthy that either the ^1P or the ^3P states of Mg are split into two A′ and one A″ components in the C_s part of the RC, which links CH_4 + Mg to CH_3–Mg–H. We only report the behavior of the lowest A′ component of each species that is correlated with the lowest energy states of CH_3–Mg–H. These curves suggest that both singlet and triplet surfaces are repulsive and exhibit a transition state (points S and P, respectively) and that a local minimum should be encountered after these points (points R′ and Q).

The geometries of the ROHF singlet and triplet transition states were optimized at the SCF 3-21G level, and these geometries were used in further Møller–Plesset calculations by method II. The resulting energies are reported in Figure 5 (points U and V). At the SCF level, no bound area is found in the Q and R′ regions. Nevertheless, with the use of a grid of points calculated by method I, a minimum is found on the singlet surface (point W). As can be seen, this point corresponds to an absolute minimum on this surface. Although no minimum appears in the triplet surface when method I is used, the triplet energy of structure W (3.19 eV), compared to that of CH_3 + MgH at 4-Å separation, indicates that a bound area actually exists in this region. Examination of the bond lengths shows that W looks essentially like a $MgH{\cdot}CH_3$ complex.

Discussion

With Li in the GS (^2S), no preference appears for either insertion or abstraction reaction, since both processes exhibit monotonous PES's and, at any rate, appear very unlikely for thermodynamic reasons. As a consequence, the reverse reaction LiH + CH_3 → CH_4 + Li is expected to be spontaneous. The PES's originating from the lowest excited 1^2P state of Li are strongly repulsive and the reaction is still endothermic, so that either a reactive diabatic or an adiabatic process equally appears very unlikely.

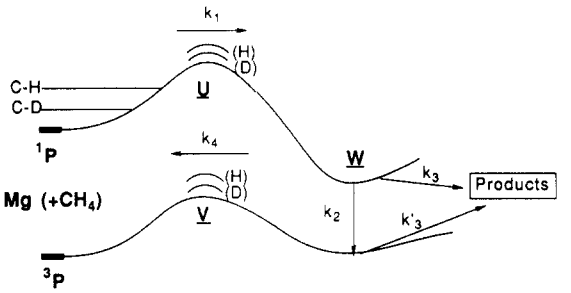

Figure 7. Qualitative kinetic scheme and isotopic effects for the Mg + CH_4 system.

With CH_4 + Mg, experimental data reported by Breckenridge et al.[6,14-16] (gas phase) and Ozin et al.[17-19] (low-temperature matrix) need to be interpreted. The measured high cross section of quenching,[16] yielding essentially chemical quenching with formation of CH_3 + MgH (gas phase) or CH_3MgH (matrix),[19] leads both authors to postulate the existence of an attractive singlet surface and little or no energy barrier along the RC. According to our calculations, at the SCF and method I levels, this surface remains weakly repulsive up to a transition state (point U, Figure 5), whereas, at the same level of calculation, an attractive surface has been found for the related Mg + H_2 system.[5] The energy barrier is rather small (0.3 eV) and would be less when the zero-point energy of the C–H bond to be broken ($\simeq$0.2 eV) is taken into account. The resulting value, ca. 0.1 eV, still appears overestimated, with respect to the experimental results, but not inconsistent, if one considers that the TS structure has been optimized at the SCF level only and thus could be improved to give a reasonably lower or even vanishing barrier. Unfortunately, such an optimization at the method II level is beyond technical possibilities, due to the size and the state of the system. The existence of a singlet bound area (point W) with a small singlet–triplet gap, in agreement with Ozin's prediction, accounts for the strong triplet Mg emission observed by this author[18] in CH_4 matrix. Reaching the ^3P emitting level requires overcoming an activation barrier (0.44 eV; point V). Nevertheless, structure W, strongly product like, could give the product upon deactivation, without overcoming any activation barrier. Such an activation is postulated by Ozin et al. to take into account the primary isotopic effect in the rate of formation of CH_3MgH observed by these authors[19] when CD_4 is used instead of CH_4. We propose a slightly different qualitative model displayed in Figure 7.

A weak energy barrier on the singlet surface (point U) could be responsible for the isotopic effect since in this structure the C–H (or C–D) bond is considerably weakened, and the zero-point energy is only $\simeq$0.15 eV for C–D, so that the frequencies associated with the normal vibrations involving this bond are smaller (Figure 7). As an end result, the k_1 constant is lower in perdeuteromethane than in methane matrices. On the other hand, on the path W → V, one can remark that the Mg–H bond is essentially unaffected, whereas the C–H bond is partially formed. Under these conditions, a "reverse" isotopic effect on the k_4 rate constant can be expected (see Figure 7). Seeing that the formation of CH_3MgH from W is a simple C–Mg bond formation, and therefore unsensitive to deuterium substitution, one may conceive that an enhanced triplet emission and a decrease in the product yield are simultaneously observed in CD_4 as Ozin did.

The production of ^3P Mg can a priori compete with product formation and especially from singlet or triplet W complexes. In the gas phase, singlet W has internal energy enough to yield CH_3 + MgH and, following Ozin, the short life of this species would not allow for singlet–triplet intersystem crossing, so that no triplet emission is detected. The separation into two fragments is the only possibility of loss of internal energy for the CH_4Mg complex, whereas, in condensed media (matrix), this energy can be transferred to the lattice, allowing the formation of the insertion product which is thermodynamically favored. The latter product

(27) Jasien, P. G.; Dykstra, C. D. *J. Am. Chem. Soc.* **1985**, *107*, 1891.
(28) Woodward, R. B.; Hoffman, R. *The Conservation of Orbital Symmetry*; Verlag Chemie, Academic Press: Weinheim, 1970.
(29) Moore, C. E. *Atomic Energy Levels*; National Bureau of Standards: Washington, DC, 1949; Vol. I.

could arise either from direct deactivation of singlet or triplet W toward the GS insertion PES or by cleavage into CH_3 and MgH and recombination of these fragments in the matrix. It can be noted that, since no significant isotopic effect is expected on the k_2 and k'_2 rate constants, such as effect could only arise from an "earlier" energy barrier, i.e., on the singlet surface.

Concerning MgH formation, it can be seen from Figure 5 that a triangular "insertion" approach is favored over the linear end-on abstraction. This result is not in complete agreement with Breckenridge's experimental results based on measurement of the rotational quantum number of nascent MgH.[14] This author found that the "low n"/"high n" ratio was 56/42. Since a high rotational quantum number is likely to arise from a triangular approach, these results would indicate a predominance of the linear abstraction mechanism. Nevertheless, we have to note that this preference is much less pronounced than in the case of the Mg + H_2 system, for which the "low n"/"high n" ratio was found equal to 13/87, indicating a large predominance of the triangular approach for the MgH formation. On the other hand, the equilibrium bond lengths of C-Mg (2.09 Å), C-H (1.08 Å), and Mg-H (1.75 Å) are such that the triangular transition state has a large C-Mg-H angle ($\simeq$120°). Hence, one can suppose that if MgH is formed in the neighboring of point U, it could have a relatively low rotational quantum number. On the other hand, if MgH is produced from the W complex having a C-H-Mg angle close to 60°, one could expect a higher rotational quantum number for this molecule. Breckenridge's results could involve a competition between both of these MgH origins.

Origin and Consequences of the Nonnuclear Attractor in the ab Initio Electron Density Functions of Dilithium

Rainer Glaser, Roy F. Waldron, and Kenneth B. Wiberg*

Department of Chemistry, Yale University, New Haven, Connecticut 06511 *(Received: July 27, 1989; In Final Form: April 19, 1990)*

Ab initio electron density functions of dilithium computed at the RHF, MP2, and CISD levels with extended basis sets and optimized bond lengths were analyzed topologically. Nonnuclear attractors were found at all levels. The nonnuclear attractor can be readily explained by the nodal properties of the valence electron density function. The analysis of their origin suggests that they might occur in long bonds of low polarity. Specific examples are cited that allow one to test this prediction. The existence of nonnuclear attractors shows that the theory of atoms in molecules does not invariably define a one-to-one relation between topologically defined basins and atoms. While the theory of atoms in molecules does not rely on such a relation, this requirement needs to be met for a chemically useful definition of atomic populations. Aside from this conclusion, the results point up a more general practical limitation of the partitioning scheme. If the electron density functions are extremely flat in the bonding region, whether a nonnuclear attractor is present or not, parameters of the topological theory that strongly depend on the locations of the partitioning surfaces might be greatly affected by the choice of the theoretical model. The crucial role is emphasized of the curvature in the direction of the bond path in judging the quality of the topological parameters of bonds of low polarity.

Introduction

The concept of *atomic properties* in molecules is one of the most useful tools for characterizing bonding and reactivity. The general problem associated with the assignment of atomic properties consists in the partitioning of the charge density, and attempts to solve it have been closely related with the progress in population analysis. Two fundamentally different approaches to population analysis have emerged in which the partitioning of the molecular electron density is done either in the Hilbert space spanned by the basis set or in real Cartesian space.[1] The latter approach has the important advantage that the partitioning of an electron density function is essentially independent of the specific characteristics, other than dimensionality, of the Hilbert space selected for the expansion of the associated wave function. In mathematical terms, the partitioning in Cartesian space is one-to-one whereas basis set partitioning is not. Methods for the partitioning in Cartesian space have been proposed in which atomic regions are defined with reference to free atoms,[2] without reference to free atoms but with other assumptions,[3] and based exclusively on the topological properties of the electron density function.[4,5] The latter probably is the most rigorous partitioning technique to date, and the topological theory of atoms in molecules[4] is based on this partitioning scheme.

The topological partitioning exploits properties of the gradient vector field of the electron density, $\nabla\rho(\mathbf{r})$. Critical points in $\nabla\rho(\mathbf{r})$, points where $\nabla\rho(\mathbf{r}) = 0$, describe the principal characteristics of the electron distribution, and they usually are classified according to the *rank*, denoting the number of nonzero eigenvalues λ_i of the Hessian matrix of $\rho(\mathbf{r})$, and the *signature*, the number of excess positive over negative eigenvalues λ_i.[6] Subspaces within $\rho(\mathbf{r})$, the basins, are defined as regions in 3D space bounded by zero-flux surfaces of $\rho(\mathbf{r})$, that is, surfaces for which $\nabla\rho(\mathbf{r})\, n(\mathbf{r}) = 0$ at all points. The space containing all of the gradient paths that terminate at one and the same nucleus defines the basin. Usually all gradient paths terminate at one of the nuclei, a (3,-3) critical point in $\rho(\mathbf{r})$, and if this were always the case, then this partitioning scheme would indeed be general in assigning atomic populations in a rigorous and chemically significant fashion. Results of recent research, however, have put into question this generality. Basins have been found that do not contain a nucleus,[7-12] and in such

(1) For a recent discussion, see: Glaser, R. *J. Comput. Chem.* **1989**, *10*, 118 and references therein.
(2) (a) Politzer, P.; Harris, R. R. *J. Am. Chem. Soc.* **1970**, *12*, 379. (b) Politzer, P.; Mulliken, R. S. *J. Chem. Phys.* **1971**, *55*, 5135. (c) Politzer, P.; Reggio, P. H. *J. Am. Chem. Soc.* **1972**, *94*, 8308. (d) Brown, R. E.; Shull, H. *Int. J. Quantum Chem.* **1968**, 663. (e) Russeger, P.; Schuster, P. *Chem. Phys. Lett.* **1973**, *19*, 254. (f) Lischka, H. *J. Am. Chem. Soc.* **1977**, *99*, 353.
(3) Wiberg, K. B. *J. Am. Chem. Soc.* **1980**, *102*, 1229.
(4) Reviews: (a) Bader, R. F. W. *Acc. Chem. Res.* **1985**, *18*, 9. (b) Bader, R. F. W.; Nygen-Dang, T. T.; Tal, Y. *Rep. Prog. Phys.* **1981**, *44*, 893.
(5) For a related method see: Streitwieser, A., Jr.; Collins, J. B.; McKelvey, J. M.; Grier, D. L.; Kohler, B. A. B.; Vorpagel, E. R.; Schriever, G. W. *Electron Distributions and the Chemical Bond*; Coppens, P., Hall, M., Eds.; Plenum Press: New York, 1982.
(6) Collard, K.; Hall, G. G. *Int. J. Quantum Chem.* **1977**, *12*, 623.
(7) Gatti, C.; Fantucci, P.; Pacchioni, G. *Theor. Chim. Acta* **1987**, *72*, 433.

0022-3654/90/2094-7357$02.50/0